

33. Radical Reactions in an X-Irradiated Phosphaalkene: a Single-Crystal ESR Study

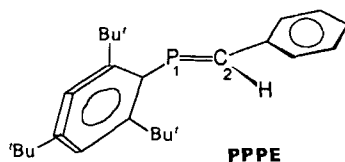
by Shrinivasa N. Bhat, Théo Berclaz, Abdelaziz Jouaiti, and Michel Geoffroy*

Département de Chimie Physique, Université de Genève, 30, quai Ernest-Ansermet, CH-1211 Genève 4

(5.VII.93)

Single crystals of 1-[2,4,6-tri(*tert*-butyl)phenyl]-2-phenylphosphaethene (**PPPE**) and of ^2D - and ^{13}C -enriched **PPPE** were studied by ESR after X-ray irradiation. Two phosphorus-centered radicals were trapped in the crystals. The first one was characterized by its ^{31}P , ^1H -, and ^{13}C -hyperfine tensors, the second one exhibited coupling with ^{31}P only. Comparison of these parameters with those predicted by *ab initio* calculations on some phosphinyl species indicates that these two radicals probably result, on the one hand, from an addition of a H-atom to the C-atom of the $\text{P}=\text{C}$ bond and, on the other, from a cyclization of the parent molecule. The proposed mechanisms are consistent with the mutual orientations of the hyperfine eigenvectors and bond directions in the undamaged molecule. A C-centered radical which results from an addition of a H-atom to the P-atom of the phosphaethylene bond is also detected.

Introduction. – Due to the numerous valence states and coordination numbers that a P-atom can exhibit, organophosphorus molecules can give rise to a large variety of radical intermediates [1]. Whereas the chemical reactions involving the formation of radicals from molecules containing a tricoordinated (*e.g.* phosphine [2]), a tetracoordinated (*e.g.* phosphine oxides [3], phosphonium salts [4]), or a pentacoordinated P-atom [5] are well documented, the generation of free radicals from molecules containing a dicoordinated phosphorus atom is much less known and has been studied only in the case of diphosphenes [6–8] and of a cyclic molecule containing a $\text{P}=\text{C}$ bond [9]. Since the pioneering studies of *Bickelhaupt* and coworkers [10], it is known that acyclic phosphaalkene molecules containing bulky substituents are stabilized by steric interaction and, for example, 1-[2,4,6-tri(*tert*-butyl)phenyl]-2-phenylphosphaethene (**PPPE**) forms crystals [11] which are rather stable at room temperature. In the present study, we will

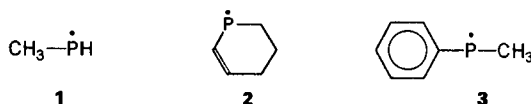


describe two mechanisms which lead to the formation of free radicals in irradiated **PPPE** and – since single-crystal ESR spectroscopy is certainly one of the most efficient methods for the identification of free radicals [12–14] – we will use this technique to investigate the nature and the structure of radiogenic radicals trapped in this material.

Experimental. – **PPPE** was synthesized following the method of Yoshifuji *et al.* [15]: after lithiation of ArPH_2 and reaction with $(t\text{-Bu})\text{Me}_2\text{SiCl}$, a subsequent lithiation led to $(t\text{-Bu})\text{Me}_2\text{Si}(\text{Li})\text{PAr}$, ($\text{Ar} = 2,4,6\text{-tri}(t\text{-butyl})\text{phenyl}$) which was reacted with benzaldehyde to yield **PPPE**. The (*E*)-isomer was obtained after separation on a silica-gel column. The deuterated compound $\text{ArP}=\text{C}(\text{D})\text{C}_6\text{D}_5$ was synthesized from $\text{C}_6\text{D}_5\text{C}(\text{D})\text{O}$ obtained from $(\text{C}_6\text{D}_5)\text{CD}_3$. $\text{ArP}=\text{C}(\text{H})(\text{C}_6\text{H}_5)$ was synthesized from $\text{C}_6\text{H}_5^{13}\text{C}(\text{H})\text{O}$ (Cambridge Isotope Laboratories). The crystal structure of **PPPE** has been determined by Appel *et al.* [11] (monoclinic, $C2/c$, $a = 41.7$, $b = 5.95$, $c = 18.68$ Å, $\beta = 98.52^\circ$).

Large single crystals were obtained by slow evaporation of solutions of **PPPE** in $\text{MeCN}/\text{Et}_2\text{O}$ 1:10 at -8° . After indexation of their faces, these crystals were irradiated at r.t. using a Philips X-rays tube (*PW1100*) equipped with a tungsten anticathode (irradiation time: 2 h, 30 kV, 30 mA). The angular variations of the ESR spectra were obtained by rotating the crystal around the c , a^* , and b axis, and by recording the ESR spectra by steps of 10° on a Bruker E-200D spectrometer (X-band, 100-kHz field modulation). These angular dependences were analyzed with a Hamiltonian which takes the electronic and nuclear Zeeman effects as well as the hyperfine interactions into account. The g tensor and the ^{31}P - and ^1H -coupling tensors were determined with an optimization program [16] which compares the positions of the experimental transitions with those calculated by second-order perturbation theory [17].

The *ab initio* calculations were performed with a 6-31G* basis set with the Gaussian 90 program [18] on a Silicon Graphics computer (Crimson model). Both the methylphosphinyl radical (1) and the six-membered ring containing a phosphinyl radical (2) were studied by the UHF method: the spin densities, the Fermi contact interaction as well as the dipolar hyperfine couplings were then obtained after spin annihilation. For the methyl(phenyl)phosphinyl radical (3), however, the $\langle S^2 \rangle$ value was found to be higher than 0.75, even after annihilation of the spin contamination; this radical was, therefore, studied by the ROHF method.



Results. – *ESR Spectra.* An example of an ESR spectrum obtained with an X-irradiated single crystal of **PPPE** is shown in Fig. 1, *b*. Two types of signals are observed in this rather complex spectrum: 1) two very anisotropic sets of intense lateral lines, 2) a central signal *C*, which, for some orientations exhibits a poorly resolved triplet structure (splitting of *ca.* 42 MHz). Additional lines, marked *X* in Fig. 1, are also detected, but their lower intensity precluded their analysis.

Due to overlap of the signals, we could not directly follow the angular dependence of the intense lines and began to study the deuterated compound $\text{ArP}=\text{C}(\text{D})\text{C}_6\text{D}_5$; this crystal led to the spectrum shown in Fig. 1, *a*, when, as for Fig. 1, *b*, the magnetic field lay in the a^*c plane and made an angle of 10° with the a^* axis. From the angular variations of the spectrum obtained with the deuterated compound, it became apparent that the sets of lateral lines were due to two radical species: the first one, called *A*, showed a large hyperfine interaction with a ^{31}P nucleus as well as an additional small coupling with a proton; the second one, called *B*, exhibited a single hyperfine splitting whose strong anisotropy was consistent with the trapping of a P-centered radical. Two different orientations of each radical (site splitting) were observed in two reference planes whereas, in accordance with the monoclinic structure of the crystal, these two orientations were equivalent in the third plane. The signal of the third species (*C*) could be clearly observed only for the orientations corresponding to a large ^{31}P -hyperfine splitting of the species *A* and *B*, for most of these orientations the deuterated compound exhibited a coupling of *ca.* 42 MHz with a spin $\frac{1}{2}$ nucleus (Fig. 1, *a*). The large linewidth ($\Gamma = 17$ MHz) was undoubtedly due to unresolved hyperfine interaction.

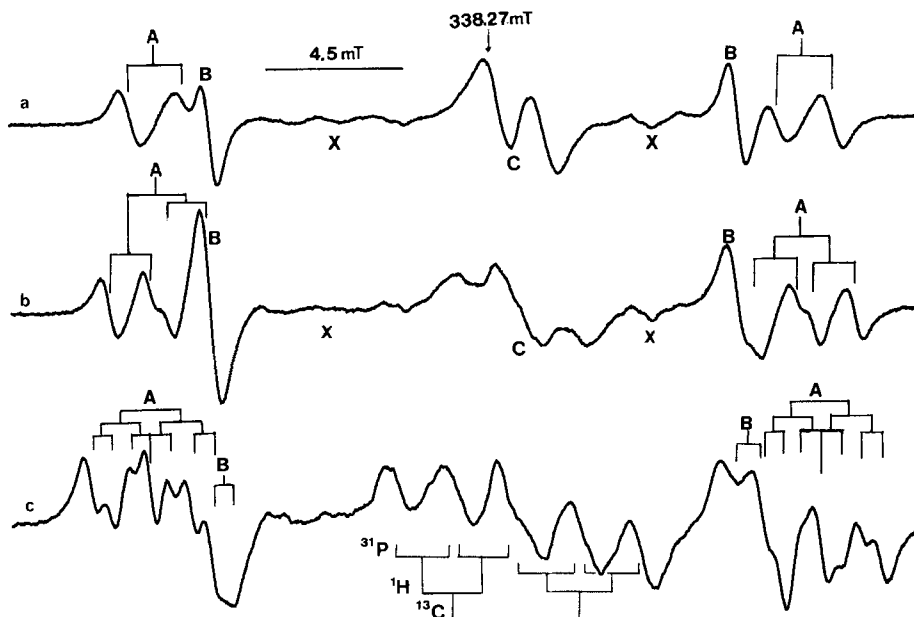


Fig. 1. a) ESR Spectrum obtained with an X-irradiated single crystal of $\text{ArP}=\text{C}(\text{D})\text{C}_6\text{D}_5$ (the magnetic field lies in the a^*c plane and makes an angle of 10° with the a^* axis). b) ESR Spectrum obtained with an X-irradiated single crystal of $\text{ArP}=\text{C}(\text{H})\text{C}_6\text{H}_5$ (same orientation as for a). c) ESR Spectrum obtained for the same orientation with a single crystal of $\text{ArP}=\text{}^{13}\text{C}(\text{H})\text{C}_6\text{H}_5$

For many orientations of the undeuterated crystal, it clearly appeared that replacing ^2D by ^1H led to an additional hyperfine splitting of *ca.* 45 MHz for the species *A*, and to the presence of a triplet pattern for the radical *C*, whereas no effect of this substitution could be detected on the spectrum of the species *B* (Fig. 1, a and b). The analysis of the angular variations of the *A* and *B* signals recorded with the undeuterated crystal is shown in Fig. 2 and leads to the tensors given in Table 1. The tensors g , ^{31}P -T and ^1H -T, obtained for the radical *A* as well as the tensors g and ^{31}P -T obtained for the radical *B* were totally consistent with those measured for the deuterated compound. For the ^{31}P -hyperfine tensor, which exhibits axial symmetry, the precision of the ‘perpendicular’ eigenvalues is rather poor (± 10 MHz); this is due to the fact that in the a^*b plane the splitting of the two sites was small, and that the separation between two experimental signals was often similar to the linewidth. Nevertheless, as shown in Fig. 2, the agreement between experimental and calculated transitions was quite satisfactory. It is worth mentioning that both the angle γ -formed between the ^{31}P -T_{||} eigenvectors of the two sites of radical *A* ($\gamma = 6^\circ$) as well as that formed between the ^{31}P -T_{||} eigenvectors of the two sites of radical *B* ($\gamma = 4^\circ$) are small and, as it will be seen below, this property is probably related to the fact that the normals **n** to the crystallographic CPC planes are almost perpendicular to the *b*-axis (**n**, $b = 80^\circ$). The lineshape of the triplet pattern observed for the radical *C* indicates that hyperfine interaction not only occurs with the two spin $\frac{1}{2}$ nuclei which exhibit a coupling of *ca.* 40 MHz, but that an interaction of *ca.* 15 MHz with an additional proton is also present (Fig. 3).

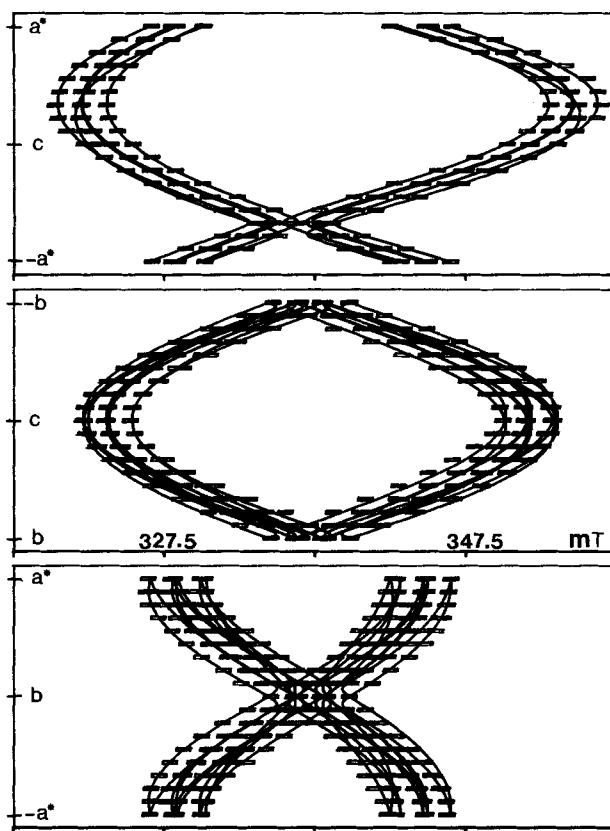


Fig. 2. Angular variations of the ESR signals A and B observed with an X-irradiated single crystal of $\text{ArP}=\text{C}(\text{H})\text{C}_6\text{H}_5$

Table 1. Experimental ESR Tensors for Phosphinyl Radicals Trapped in an X-Irradiated Single Crystal of PPPE

Tensor		Eigenvalues	Eigenvectors		
			/a	/b	/c*
Radical A					
g-tensor	g ₁	2.0016	+ 0.3352	∓ 0.1873	+ 0.9232
	g ₂	2.0065	+ 0.3027	± 0.9494	+ 0.0826
	g ₃	2.0145	+ 0.8920	∓ 0.2518	− 0.3749
T(³¹ P) [MHz]	T ₁	20	− 0.0456	∓ 0.9982	− 0.0364
	T ₂	65	− 0.9250	± 0.0284	+ 0.3784
	T ₃	915	− 0.3767	± 0.0510	− 0.9248
T(¹ H _a) [MHz]	T' ₁	43	0.1945	± 0.5732	+ 0.7958
	T' ₂	51	− 0.8895	∓ 0.2385	0.3893
	T' ₃	54	− 0.4129	± 0.7838	− 0.4635
T(¹ H _b) [MHz]	T'' ₁	40	− 0.8401	∓ 0.0846	+ 0.5354
	T'' ₂	43	+ 0.4408	± 0.4678	+ 0.7658
	T'' ₃	52	+ 0.3152	∓ 0.8797	+ 0.3557

Table 1 (cont.)

Tensor		Eigenvalues	Eigenvectors		
			/a	/b	/c*
Radical <i>B</i>					
g-tensor	g ₁	2.0008	+ 0.2734	∓ 0.3880	+ 0.8801
	g ₂	2.0072	− 0.0559	± 0.9070	+ 0.4172
	g ₃	2.0136	− 0.9602	∓ 0.1632	+ 0.2263
T(³¹ P) [MHz]	T ₁	39	+ 0.6928	± 0.7086	− 0.1326
	T ₂	65	+ 0.6854	∓ 0.7046	− 0.1831
	T ₃	939	+ 0.2232	∓ 0.0359	+ 0.9740

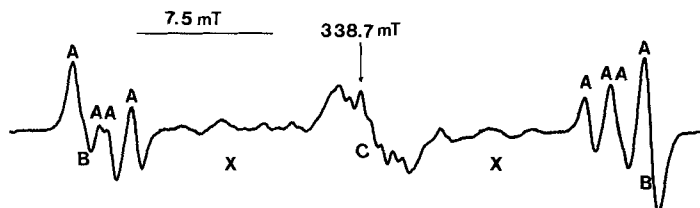


Fig. 3. ESR Spectrum obtained with an X-irradiated single crystal of $\text{ArP}=\text{C}(\text{H})\text{C}_6\text{H}_5$, when the magnetic field is aligned along the *c* axis

The ESR spectra obtained for the species *A* with $\text{ArP}=\text{C}(\text{H})\text{C}_6\text{H}_5$ exhibited an additional splitting of 17 MHz (Fig. 1, *c*) which was not dependent upon the orientation of the magnetic field. For few orientations of the crystal, a similar coupling (ca. 17 MHz) was also observed for the radical *B*; it was, however, impossible to follow the angular variation of this latter ^{13}C splitting because, for many orientations of the magnetic field, the corresponding four lines (two sites, one ^{13}C coupling) were overlapped by the numerous lines of radical *A* (two sites, two ^1H couplings, one ^{13}C coupling). For many orientations of the crystal, the ^{13}C enrichment led to a drastic modification of the spectrum due to the *C* species (Fig. 1, *c*): a very anisotropic coupling with a spin $\frac{1}{2}$ was detected and the maximum of this interaction (ca. 182 MHz) was observed in the region corresponding to the maximum ^{31}P splitting of radicals *A* and *B*. Unfortunately, the angular variation of these signals could not be followed with enough precision, and the ^{13}C hyperfine eigenvalues could not be determined for radical *C*.

Ab initio Calculations. To interpret the ESR spectra due to a phosphinyl species, we first used *ab initio* calculations (UHF method) to predict the hyperfine couplings of the methylphosphinyl radical (**1**; $\langle S^2 \rangle = 0.75$ after annihilation of the spin contamination). In the fully optimized geometry of **1** ($\angle \text{HPC} = 96.30^\circ$, $\text{P}-\text{C} = 1.860 \text{ \AA}$) a $\text{C}-\text{H}$ bond lies in the molecular $\text{H}-\text{P}-\text{C}$ plane and, as expected [19], the unpaired electron is mainly confined to a phosphorus p_π orbital ($\rho_{3p} = 0.61$). The rotation of the Me group about the $\text{P}-\text{C}$ bond corresponds to a very low barrier ($1.43 \text{ kcal} \cdot \text{mol}^{-1}$) and the dependence of the various isotropic coupling constants upon the dihedral angle θ formed between the plane containing the phosphorus $3p_\pi$ orbital, and one of the three $\text{C}-\text{H}$ bonds is shown in Fig. 4. The dipolar constants are not very sensitive to the orientation of the Me group ($565 \text{ MHz} < ^{31}\text{P}-\tau_\parallel < 566 \text{ MHz}$, $6.0 \text{ MHz} < ^1\text{H}(\text{Me})-\tau_{\text{max}} < 7.05 \text{ MHz}$, $1.97 \text{ MHz} < ^{13}\text{C}-\tau_{\text{max}} < 2.00 \text{ MHz}$).

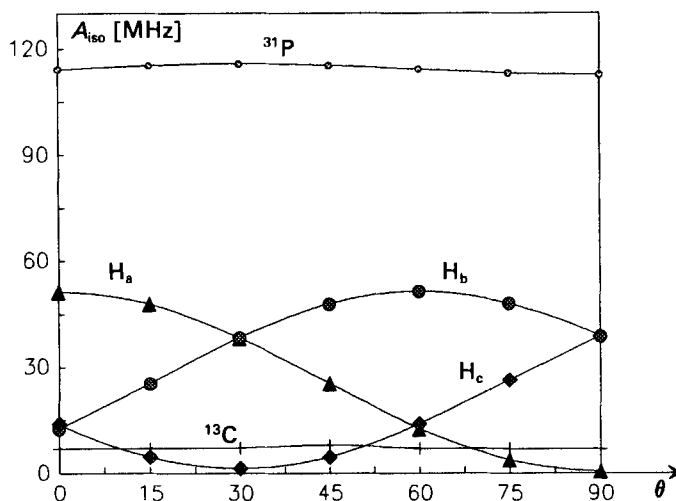


Fig. 4. Calculated variation of the isotropic ^{13}C , ^{31}P , and Me protons couplings for the methylphosphinyl radical **1** as a function of the dihedral angle θ formed between the semi-occupied phosphorus p_π orbital and the CH_a bond of the Me group

The energies and spin densities of radical **3** were calculated by using the ROHF method (*vide supra*). The geometry of the Ph ring and of the Me group were fixed and a C–H bond of the Me moiety was maintained in the C–P–C plane; the C–P–C angle, the Ph–P and the P–Me distances were then optimized for various values of the dihedral angle α formed by the C–P–C plane and the Ph plane. These calculations showed that the energy of **3** is only very slightly dependent upon this dihedral angle α (rotation barrier equal to $1.25 \text{ kcal}\cdot\text{mol}^{-1}$). The minimum energy is obtained, when these two planes coincide ($\angle \text{C–P–C} = 103.59^\circ$, $\text{Ph–P} = 1.838 \text{ \AA}$, $\text{P–Me} = 1.855 \text{ \AA}$), and the spin density in the phosphorus p_π is then equal to 0.91; this spin density is almost completely insensitive to the orientation of the plane of the Ph ring.

After annihilation of the spin contamination, the $\langle S^2 \rangle$ value found by the UHF method for the fully optimized geometry of **2** is equal to 0.759. This six-membered ring, which contains both a phosphinyl group and a C=C bond, adopts the half-boat conformation [20] shown in Fig. 5 ($\text{C}(6)\text{–P} = 1.866 \text{ \AA}$, $\text{P–C}(2) = 1.774 \text{ \AA}$, $\text{C}(3)\text{–C}(2) = 1.366 \text{ \AA}$,

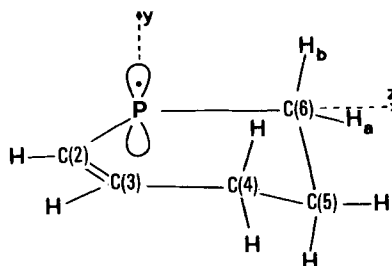


Fig. 5. Optimized structure of radical **2** (UHF calculations)

$C(4)-C(3) = 1.507 \text{ \AA}$, $C(5)-C(4) = 1.530 \text{ \AA}$, $C(6)-C(5) = 1.531 \text{ \AA}$, $\angle C(6)-P-C(2) = 99.98^\circ$, $\angle C(3)-C(2)-P = 126.9^\circ$, dihedral angles: $C(4)-C(3)-C(2)P = -2.4^\circ$, $C(3)-C(2)-P-C(6) = -2.0^\circ$, $P-C(6)-C(5)-C(4) = -61.3^\circ$. This geometry allows the phosphorus semi-occupied orbital to be aligned along the π orbitals of the $C=C$ bond and confers an allylic character to the radical **2**: the unpaired electron is delocalized on both the P- ($\rho_{P,py} = 0.74$) and the C(3)-atom ($\rho_{C(3),py} = 0.38$), moreover the spin density on the central atom is negative ($\rho_{C(2),py} = -0.15$). Nevertheless, as shown in Table 2, the ^{31}P -hyperfine interaction remains very similar to that usually observed for phosphinyl radicals while the adjacent CH_2 group $C(6)\text{H}_a\text{H}_b$ exhibits a small ^{13}C coupling ($\sim 6 \text{ MHz}$) and two very different ^1H isotropic constants which reflect significant differences in the dihedral angles ($C(2)-P-C(6)-\text{H}_a = 155.4^\circ$, $C(2)-P-C(6)-\text{H}_b = -90.2^\circ$).

Table 2. Calculated Hyperfine Couplings for **2** (reference axes given in Fig. 5)

Nucleus	Isotropic coupling [MHz]	Anisotropic coupling			
		Eigenvalues [MHz]	Eigenvectors		
			/x	/y	/z
^{31}P	122	433	0.0158	0.9998	0.0150
		-224	0.5773	-0.0214	0.8163
		-209	0.8164	-0.0042	-0.5775
$^{13}\text{C}(2)$	6	-1	0.9939	-0.0910	-0.0620
		0	0.0393	-0.2328	0.9717
		1	0.1029	0.9683	0.2278
$^1\text{H}_b$	35	5	-0.4288	-0.0841	0.8995
		-3	0.8381	0.3347	0.4308
		-2	-0.3373	0.9386	-0.0730
$^1\text{H}_a$	8	-3	0.9059	0.4152	-0.0832
		-2	0.4181	-0.8460	0.3308
		5	-0.0670	0.3344	0.9400

Discussion. – *Identification of the Radical Species.* The isotropic and anisotropic ^{31}P -hyperfine constants given in Table 3 have been obtained by assuming that the eigenvalues shown in Table 1 are positive. Comparison with the atomic values calculated by Morton and Preston [21] leads to the spin densities which are also shown in Table 3.

Table 3. Experimental Isotropic and Anisotropic Hyperfine Couplings for Radicals A and B

	Isotropic coupling [MHz]	Dipolar coupling [MHz]			s-Spin density	p-Spin density
		τ_1	τ_2	τ_3		
Radical <i>A</i>						
^{31}P	333	-313	-268	581	0.02	0.79
$^1\text{H}_a$	49	-6	2	5		
$^1\text{H}_b$	45	-5	-2	7		
Radical <i>B</i>						
^{31}P	348	-309	-283	591	0.03	0.80

For both radicals *A* and *B*, the strong localization of the unpaired electron in a phosphorus p-orbital suggests that two phosphinyl species have been trapped in the crystal [19]. The isotropic ^{31}P coupling calculated by *ab initio* methods for the equilibrium geometry of HPMe is lower than the two experimental constants; however, the difference between the calculated (122 MHz) and the measured values (330 MHz for radical *A* and 347 MHz for radical *B*) corresponds, in fact, to a difference of only 0.01 in terms of 3s spin densities. Since correlation between experimental and theoretical spin densities is seldom better than ± 0.05 , this difference between the theoretical and experimental values of the 3s spin densities in the ^{31}P -atom is not significant. The agreement on the dipolar coupling is very satisfactory ($\tau_{\text{exp,radical } A} = 581 \text{ MHz}$, $\tau_{\text{exp,radical } B} = 592 \text{ MHz}$, $\tau_{\text{calculated}} = 565 \text{ MHz}$) and confirms the identification of a phosphinyl species for both radicals *A* and *B*.

The two proton couplings measured for the radical *A* are almost equal and are characterized by a low anisotropy which, *a priori*, is consistent with their being due to H-atoms located in β -position from the radical centre. As shown on Fig. 4, two isotropic couplings close to 40 MHz are indeed calculated for HPMe when C–H_a and C–H_b make a dihedral angle of 30° and 150°, respectively, with the phosphorus 3p_x direction. The fact that deuteration of the C-atom of the phosphalkene group results in the suppression of one of the two proton couplings indicates that the radical *A* is probably produced by the addition of a H \cdot atom to the C-atom of the P=C bond. This conclusion is totally consistent with the value of the ^{13}C coupling calculated for the Me group in the methylphosphinyl radical **1**: as found experimentally, the anisotropy of this interaction is very small, and the isotropic coupling is less than 10 MHz. The conformation of radical *A* is shown in Fig. 6.

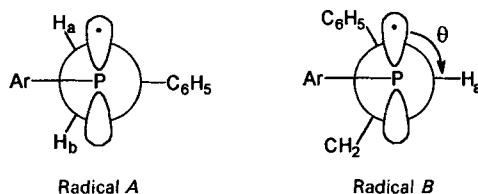


Fig. 6. Conformations of the two phosphinyl radicals *A* and *B*

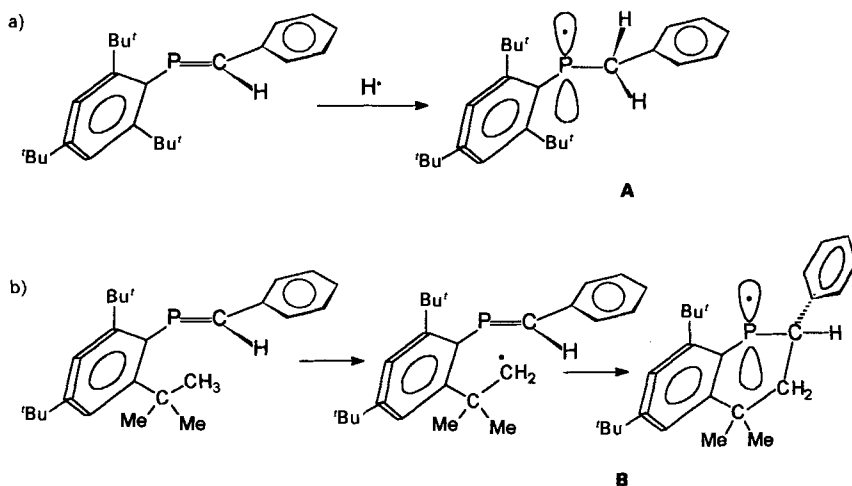
A major difference between radical *B* and radical *A* lies in the absence of any proton coupling for the radical *B*; however, both the ^{13}C and the ^{31}P couplings indicate that the radical *B* also results from an addition on the phosphalkene C-atom. The most reasonable interpretation of the *B* spectrum is, therefore, that cyclization of PPPE leads to a phosphinyl radical which contains only one H-atom in the β -position from the P-atom, and that the corresponding dihedral angle θ (Fig. 6), near 90°, implies a hyperfine splitting close to zero. As shown in Table 2, the hyperfine eigenvalues predicted by *ab initio* calculations for the radical **2** are consistent with the couplings measured for radical *B*.

Although the hyperfine tensors could not be determined for the radical *C*, the anisotropic ^{13}C splitting is consistent with a high spin density on the C-atom C(2), moreover, for several orientations, additional anisotropic couplings with two spin $\frac{1}{2}$ nuclei are clearly observed. This pattern is reminiscent of previous results for

$\text{Ph}_3\text{P}^+-^{13}\text{CH}_2$ [4] (^{13}C -T: 42 MHz, 28 MHz, 229 MHz; ^1H -T: 33 MHz, 92 MHz, 58 MHz; ^{31}P -T: 120 MHz, 106 MHz, 106 MHz), it is, therefore, plausible that these two additional anisotropic couplings are due to a H- and a P-nucleus located in the α -position from the radical C-atom, and that the signals C are due to $\text{Ar}(\text{R})\text{PC}(\text{H})\text{Ph}$.

Radical Mechanism. The crucial event in the radiolysis of **PPPE** is certainly the homolytic scission of a C–H bond of a *t*-Bu moiety. After diffusion in the crystal matrix, the H \cdot probably adds to the phosphalkene C-atom of a neighboring molecule and forms the radical **A** as shown in *Scheme 1, a*. However, if the rupture of a C–H bond occurs on one of the two Me groups located close to the P=C bond (the crystal structure shows that the corresponding $\text{C}(\text{CH}_3) \cdots \text{C}(\text{C}=\text{P})$ distance is $\sim 3 \text{ \AA}$) the resulting $\dot{\text{C}}\text{H}_2$ group attacks the phosphalkene C-atom and gives rise to the radical **B** (*Scheme 1, b*).

Scheme 1



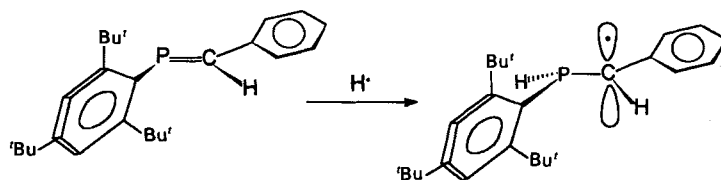
We will now try to improve the description of this process by comparing the orientation of the hyperfine eigenvectors with the crystallographic bond directions of the undamaged molecule. The crystal structure of **PPPE** [11] shows that the Ph ring bound to the phosphalkene C-atom and the P=CH moiety are practically coplanar, whereas the Ar ring bound to the P-atom is oriented perpendicular to the P–C–H plane (the corresponding dihedral angle is 92.9°); the C–P–C bond angle is 100.9° . In a phosphinyl radical, the direction of the phosphorus $3p_x$ -orbital is oriented perpendicular to the C–P–C plane and is given by the ^{31}P - τ_{\parallel} eigenvector. For the radical **A**, whatever pairing between the crystallographic site and the radical site is chosen, the ^{31}P - τ_{\parallel} eigenvector makes a small angle with the normal to the crystallographic C–P–C planes: 11° for one site, 15° for the other. Such small angles indicate that the C–P–C plane of the precursor is almost unaffected by the formation of the radical. Furthermore, the fact that the two proton couplings are quite similar shows that, following the addition of the H \cdot atom, the Ph ring bound to the C-atom of the P=C bond probably remains in this C–P–C plane which becomes the bisector of the new H–C–H moiety. This lack of drastic rearrange-

ment in the geometry of the phosphalkene molecule is not surprising, since the presence of the bulky *t*-Bu groups hinders the rotation around the Ar–P bond [8]; it is, therefore, quite plausible that, in the phosphinyl radical **A**, the phosphorus semi-occupied $3p_\pi$ orbital remains oriented parallel to the plane of the aromatic moiety Ar, while the *ab initio* calculations predict that **3** is very slightly stabilized when the C–P–C and Ph planes are coplanar (*vide supra*).

Since the $^{31}\text{P}-\tau_{\parallel}$ eigenvector of radical **B** is practically parallel to that of radical **A** ($^{31}\text{P}-\tau_{\parallel}(\text{radical A}), ^{31}\text{P}-\tau_{\parallel}(\text{radical B}) = 9^\circ$), the formation of radical **B** is also not accompanied by a drastic reorientation of the C–P–C plane; in this case, however, it is probable that the cyclization process implies a rotation of the aromatic ring around the Ar–P bond and that the resulting six-membered ring can adopt a conformation close to the half-boat geometry predicted for **2** by *ab initio* calculations. The fact that the C–H bond located in the β -position from the P-atom lies in the C–P–C plane (the corresponding ^1H -isotropic coupling constant is not observed) indicates that the Ph ring bound to the phosphalkene C-atom undergoes a considerable reorientation during the intramolecular rearrangement. Unfortunately, it is impossible to know if both *t*-Bu groups located *ortho* to the P-atom participate in the reaction, since in each case the semi-occupied orbital of the resulting radical is expected to be oriented along the normal to the original C–P–C plane.

The C-centered radical **C** probably results from a radical addition to the P-atom (Scheme 2). This process is similar to a radical reaction previously observed with a diphosphene compound [7] [8]. Although the spectra are rather complex (two sites are also expected for this species), their line shapes are more consistent with the addition of an H-atom than with a cyclization process.

Scheme 2



In summary, the addition of a radical to a phosphalkene in the solid state can take place equally well on the C-atom as on the P-atom of the P=C bond. In the former case, phosphinyl radicals are generated, while in the second case a phosphomethyl radical is produced. In both cases, the resulting radical intermediates are stable enough to be observed at room temperature.

The authors thank Dr. G. Bernardinelli for indexation of the faces of the crystals studied by ESR. This work was supported by the Swiss National Science Foundation.

REFERENCES

- [1] W. G. Bentrude, in 'Free Radical', Ed. J. K. Kochi, J. Wiley, New York, 1973, Vol. 2, p. 595–664.
- [2] P. Tordo, in 'The Chemistry of Organophosphorus Compounds' Ed. F. R. Hartley, Series 'The Chemistry of Functional Groups', Ed. S. Patai, J. Wiley, Chichester, 1990, p. 137–149.
- [3] D. Nelson, M. C. R. Symons, *J. Chem. Soc., Perkin Trans. 2* **1977**, 286.
- [4] M. Geoffroy, L. Ginet, E. A. C. Lucken, *Mol. Phys.* **1977**, *34*, 1175.
- [5] J. H. M. Hamerlinck, P. Schipper, H. M. Buck, *J. Am. Chem. Soc.* **1983**, *105*, 385.
- [6] B. Cetinkaya, A. Hudson, M. F. Lappert, H. Goldwhite, *J. Chem. Soc., Chem. Commun.* **1982**, 609.
- [7] M. Cattani-Lorente, M. Geoffroy, *J. Chem. Phys.* **1989**, *91*, 1498.
- [8] M. Geoffroy, M. Cattani-Lorente, *J. Chim. Phys.* **1991**, *88*, 1159.
- [9] M. Geoffroy, G. Terron, G. Bernardinelli, *Chem. Phys. Lett.* **1991**, *182*, 242.
- [10] Th. C. Klebach, R. Lonrens, F. Bickelhaupt, *J. Am. Chem. Soc.* **1978**, *100*, 4886.
- [11] R. Appel, J. Menzel, F. Knoch, P. Volz, *Z. Anorg. Allg. Chem.* **1986**, *534*, 100.
- [12] T. Berclaz, M. Geoffroy, *Helv. Chim. Acta* **1978**, *61*, 684.
- [13] M. Geoffroy, A. Llinares, J. R. Morton, *Helv. Chim. Acta* **1983**, *66*, 673.
- [14] M. Cattani-Lorente, G. Bernardinelli, M. Geoffroy, *Helv. Chim. Acta* **1987**, *70*, 1897.
- [15] M. Yoshifuji, K. Toyota, N. Inamoto, *Tetrahedron Lett.* **1985**, *26*, 1727.
- [16] F. James, M. Roos, CERN Program Library, CERN, Geneva, Switzerland, 1976.
- [17] M. Iwasaki, *J. Magn. Reson.* **1974**, *16*, 417.
- [18] F. M. J. Frisch, M. Head-Gordon, G. W. Trucks, J. B. Foresman, H. B. Schlegel, K. Raghavachari, M. Robb, J. S. Binkley, C. Gonzalez, D. J. Defrees, D. J. Fox, R. A. Whiteside, R. Seeger, C. F. Melius, J. Baker, R. L. Martin, L. R. Kahn, J. J. P. Stewart, S. Topiol and J. A. Pople. Gaussian 90, Gaussian Inc., Pittsburg PA, 1990.
- [19] M. Geoffroy, E. A. C. Lucken, C. Mazeline, *Mol. Phys.* **1974**, *28*, 839.
- [20] D. Cremer and J. A. Pople, *J. Am. Chem. Soc.* **1975**, *97*, 1354.
- [21] J. R. Morton and K. F. Preston, *J. Magn. Reson.* **1978**, *30*, 577.